Attachment 16

10 River Plume Dynamics in the Central Great Barrier Reef

Brian King, Felicity McAllister, Eric Wolanski, Terry Done, and Simon Spagnol

CONTENTS

INTRODUCTION

Rivers collect the freshwater runoff from the land and deliver it to the sea at the coast. The runoff also collects and carries sediment, nutrients, and contaminants depending on the catchment characteristics and land uses. Once discharged from the river, the runoff drives a buoyant plume into coastal and shelf waters. The plume eventually spreads and mixes and moves around with the winds and currents. This mixing with ambient coastal waters will ultimately dilute the runoff plume as well as any concentrations of sediments, nutrients, and contaminants carried within the plume. In the wet and dry tropical catchments adjoining the Great Barrier Reef (GBR), river discharges are highly seasonal and usually event-driven in nature and result from rainfall events associated with evolving monsoon troughs or passing tropical cyclones (Wolanski, 1994).

0-8493-0833-X/01/$0.00+$.50

The unpredictable nature of rainfall and runoff events, and the unsteadiness and patchiness of the resulting plume intrusions in a complex region such as the GBR have traditionally made data logistically difficult to collect. Direct rainfall inputs onto the shelf can also lower surface salinity significantly (Wolanski, 1994) and at a time when river discharges are also significant. Thus large spatial mapping of salinities was needed to determine the origins of lower salinity events (<34 ppt) within the reef matrix of the GBR. Further, understanding the possible fates of river plumes is a key question for the management of the GBR because of their ability to transport pollutants from human activities on land into the GBR Marine Park.

Evidence of significant plume intrusion into the GBR has been observed and measured. Wolanski and Ruddick (1981) and Wolanski et al. (1997) showed that under favourable wind conditions, the plume waters from the Fly River do intrude into the northern GBR Marine Park at times. O'Neill et al. (1992) measured the flood plume from the Fitzroy River after the passage of Cyclone Joy in 1991. Using a combination of salinity measurements and aerial observations of water colour, O'Neill et al. (1992) mapped the 12-day travel of the Fitzroy River Plume from Keppel Bay into the Capricorn Bunker Group of reefs in the Southern GBR. Ayukai et al. (1997) mapped the salinity and nutrient distributions of the Daintree River plume into GBR waters after the passage of Cyclone Sadie. Wolanski and Van Senden (1983) reported the most detailed survey to date, which covered the 1981 flood events from the Burdekin, Herbert, Tully, Johnstone, and Barron Rivers. King et al. (1998) utilized this survey to calibrate and verify a three-dimensional hydrodynamic model of the Burdekin River in flood. The model was used to produce a comprehensive long-term time varying and three-dimensional spatially varying database of the fate and mixing of plume waters from the Burdekin, Herbert, Tully, and South Johnstone Rivers (King et al., 2000; McAllister et al., 2000).

Animations of the predicted plumes from 1973 to 1998 were created from the model outputs to detail the dynamics of these river plumes. The animations also show some of the events that lead to an intrusion of river plumes into reef waters. This database was ultimately analysed to map the return periods of the likely impacts of runoff from these major rivers to nearby reefs (King et al., 2000). This analysis provided stakeholders with a spatial and temporal summary risk assessment of river plumes in the central section of the GBR. Here, data from the field and some of the model simulations are presented to demonstrate some of the event dynamics and known characteristics of river plumes in the central section of the GBR.

DISCHARGE CHARACTERISTICS OF THE CENTRAL GBR REGION

The rainfall catchment area adjoining and impacting the GBR Marine Park totals 424,000 km^2 not including the influence from rivers intruding into the GBR from Papua New Guinea and Irian Jaya. The mainland catchments have been divided into 35 drainage basins. The two largest basins in this region are the Burdekin and Fitzroy river systems, which make up two thirds of the total watershed area draining into the GBR.

In particular, the Burdekin River has a catchment area of 130,000 km^2, which is equivalent to the land area of Greece. This river has the largest recorded mean annual flow (approximately 9.7 billion m^3/year) for any river adjacent to the world heritage-listed GBR (Wolanski, 1994). The river mouth is located between Cape Upstart to the south and Cape Bowling Green to the north (Figure 1). The runoff, while extensive, is also highly variable, limited to the occasional flood event (0 to 3 per year) usually occurring during the Austral summer months of December to March.

Daily discharge data from the Burdekin River since 1951 demonstrate the decadal, annual, and inter-annual temporal variability associated with runoff events in the Central GBR region. These data were also summed to give a total volume discharged for each water year (July through June) and then ranked from largest to smallest values. From the ranking, return periods based on the total volume of freshwater discharged by the Burdekin River over the last 47 years were estimated using a Pearson III Type Distribution (ARA, 1998) and are given in Table 1. From Table 1, it can be seen that the wet season of 1973–1974 was an unusually large event. An event of this magnitude is estimated to have a likely return period of once every 79 years.

In contrast, the catchment areas farther north of the Burdekin lie within more rugged and mountainous terrain resulting in more river systems transversing the region draining significantly smaller catchments. The major river systems here are the Herbert, Tully, and Johnstone Rivers (see Figure 1). Note that as a result of the Burdekin's significantly larger catchment size, its annual discharge volumes almost always exceed those of the Herbert, Tully, and Johnstone Rivers (Figure 2). Figure 2 shows that there were a considerable number of years when discharge from the river was negligible, such as 1994–1995, 1992–1993, 1991–1992, 1986–1987, 1984–1985, and 1981–1982. Figure 3 shows a comparison between the discharge hydrographs (flow rates) for the Burdekin, Herbert, Tully, and Johnstone Rivers for the wet season ending 1986 and 1981 demonstrating the spatial and temporal variability inherent in the flow rates from the major rivers of the Central GBR. The rainfall event most influencing the 1986 hydrographs was due to the passage of Cyclone Winifred over all catchments (Puotinen et al., 1997). Figure 3b shows that three significant rainfall events occurred in 1981. The first two events resulted from the presence of the monsoon trough over all catchments, while the last event was associated with tropical cyclone Freda.

MODELLING RIVER PLUMES IN THE CENTRAL GBR REGION

King et al. (1998) calibrated and verified a three-dimensional hydrodynamic model of the Burdekin River in flood. The model was used to produce a comprehensive long-term time varying and three-dimensional spatially varying database of the fate and mixing of plume waters from the Burdekin, Herbert, Tully, and South Johnstone Rivers (King et al., 2000; McAllister et al., 2000).

King et al. (1998) used the "MECCA" three-dimensional hydrodynamic model (see Hess, 1989) from NOAA, which incorporated river plume dynamics into the

TABLE 1
Return Periods and Annual Exceedence Probabilities (AEP %) Calculated for the Total Volume of Freshwater Discharged by the Burdekin River for 47 Water Years

Rank	Water Year	Discharge (megalitres)	AEP (%)	Return Period
1	1973–1974	53,878,655	1.27	78.7
2	1990–1991	40,411,687	3.39	29.5
3	1957–1958	28,068.886	5.51	18.2
4	1954–1955	24,146,521	7.63	13.1
5	1955–1956	22,105,966	9.75	10.3
6	1953–1954	21,018,573	11.86	8.4
7	1971–1972	18,897,175	13.98	7.2
8	1980–1981	17,967,853	16.10	6.2
9	1967–1968	16,095,218	18.22	5.5
10	1978–1979	15,590,866	20.34	4.9
11	1975–1976	11,828,423	22.46	4.5
12	1952–1953	10,968,693	24.58	4.1
13	1956–1957	9,859,008	26.69	3.7
14	1962–1963	9,690,007	28.81	3.5
15	1989–1990	9,529,963	30.93	3.2
16	1988–1989	9,056,236	33.05	3.0
17	1982–1983	8,758,709	35.17	2.8
18	1996–1997	8,703,774	37.29	2.7
19	1976–1977	8,565,482	39.41	2.5
20	1974–1975	8,482,719	41.53	2.4
21	1997–1998	8,047,517	43.64	2.3
22	1970–1971	6,136,544	45.76	2.2
23	1958–1959	6,002,436	47.88	2.1
24	1983–1984	5,287,534	50.00	2.0
25	1977–1978	5,170,492	52.12	1.9
26	1959–1960	5,026,967	54.24	1.8
27	1969–1970	4,856,183	56.36	1.8
28	1979–1980	4,675,890	58.47	1.7
29	1985–1986	3,801,182	60.59	1.7
30	1987–1988	3,791,881	62.71	1.6
31	1964–1965	3,747,057	64.83	1.5
32	1972–1973	3,603,037	66.95	1.5
33	1993–1994	2,906,115	69.07	1.4
34	1961–1962	2,623,611	71.19	1.4
35	1966–1967	2,404,477	73.31	1.4
36	1981–1982	2,330,380	75.42	1.3
37	1965–1966	2,204,311	77.54	1.3
38	1995–1996	1,847,753	79.66	1.3
39	1963–1964	1,787,876	81.78	1.2
40	1984–1985	1,352,955	83.90	1.2
41	1960–1961	1,341,715	86.02	1.2
42	1951–1952	931,768	88.14	1.1
43	1994–1995	794,576	90.25	1.1
44	1986–1987	579,662	92.37	1.1
45	1992–1993	561,551	94.49	1.1
46	1991–1992	509,291	96.61	1.0
47	1968–1969	351,184	98.73	1.0

model's governing three-dimensional equations. The model was designed to predict tidal, wind, and density-driven flows in bays and on continental shelves. MECCA has been extensively applied to study the salinity and temperature distribution in Chesapeake Bay and surrounding shelf areas (Hess, 1986).

The MECCA model uses a three-dimensional grid to mathematically represent elements of the water column within the study region. King et al. (1998) designed a grid that covered the entire shelf of the central section of the GBR from Cairns to Bowen (see Figure 1). The numerical grid representing the domain had over 100,000 computational points, that is, 5 layers in the vertical, 211 points in the along-shelf direction, and 95 in the across-shelf direction. The grid elements spacing in the horizontal plane were 2 km × 2 km throughout, while the vertical grid spacing varied according to the depth (sigma representation). For example, depths near the coast were of the order of 5 to 10 m, thus the vertical grid spacing would be 1 to 2 m, respectively. While current computer hardware limitations prevent the use of a finer grid at this stage, the 2-km resolution of the bathymetry is sufficient to represent the individual reefs of the GBR in this region.

The model was initially set up to simulate a flood of freshwater from the Burdekin River into the coastal waters of the GBR. King et al. (1998) verified this model for the entire 1981 flood event. This was achieved by forcing the model to incorporate the daily variability in the river's discharge and actual wind data (at 3 hourly intervals), against the historical field salinities reported in Wolanski and Van Senden (1983). Comparisons between model results and field data for three different days of field surveys show very good agreement between the observed and predicted salinity distribution in coastal waters at corresponding times. King et al. (1998) also undertook sensitivity analysis on the 1981 model simulations. The model showed that the main driving influences on the fate of the plume water were the discharge volume of the river (in the near field, that is, less than 100 km from the mouth) and the local wind forcing in the far field. Thus, each year, one would expect different plume trajectories depending on the time-varying nature of both the wind and the rainfall.

The time-step of the model was set to simulate the river dynamics at 30-s intervals. Such high temporal resolution was required to ensure the correct representation of the buoyancy terms, since discharge rates from the Burdekin can exceed 25,000 m^3/s at times.

Wind data (at 3-h intervals) were obtained from either the nearby Mackay weather station or from the nearby AIMS weather station.

Ambient salinity levels in the GBR fluctuate due to a number of processes such as offshore oceanic upwelling events and direct rainfall. Wolanski (1994) shows that 35 ppt is typical for waters in the GBR, and hence, 35 ppt was defined within the model as the background salinity. Hence, the model calculated the mixing of Burdekin freshwater with oceanic water and calculated a resulting salinity for each cell. A salinity of 0 ppt is all freshwater, a salinity of 17.5 ppt is an even mix of freshwater and seawater, a 31.5 ppt means a 10% content of freshwater present, and a 33.5 ppt contains less than 5% freshwater. Regions of 35 ppt within the model domain contain no freshwater.

Daily discharge data for each river were obtained from the Queensland Water Resources Commission and supplied to the model for each simulation.

SIMULATING THE 1981 FLOOD EVENT

The discharge data for 1981 (Figure 3a) shows that three separate flood events occurred. The total volume of freshwater discharged into the GBR from the Burdekin River catchment area at this time was a massive 18 billion tonnes (or 18 km^3) of water. Table 1 shows that this volume corresponds to an event that has an expected annual return period of every 6.2 years. King et al. (1998) simulated the entire 1981 flood event period from 1 January, 1981 until 31 March, 1981.

Animation 1 shows the evolution of the Burdekin flood plume. Note that as the first discharge for the season begins, the plume begins to form and turns left at the mouth, a result of the effects of the Coriolis Force in the Southern hemisphere (that is, due to the Earth's rotational effects), and flows northward along the coast. On day 23 (24 January, 1981), the river reached the peak discharge of this flood at 12,000 m^{3}s^{-1}. The wind vector at this time showed that the wind was strong and from the SE at 10 m s^{-1}. As a result of both these conditions, freshwater filled the entire Upstart Bay and a tongue of the brackish water (<30 ppt) stretched 150 km northward along the coast to reach Palm Island. This extensive excursion by plume waters is driven both by the SE winds and the massive strength of the river's discharge.

The plume often touches the bottom in the shallow coastal regions (depth <15 m) depending on wind and discharge rate. As it spreads offshore, its freshwater content will most likely make it more buoyant than deeper offshore waters. This buoyancy difference further drives movement of the plume. This buoyancy-driven, across-shelf current will be a function on the density gradients across the shelf at the time. Hence the plume floats and generates a stratified water column in the deeper coastal waters along the marked transect. At the end of the first and major discharge event, the SE winds weakened at this time, though they had advected the plume and the 30-ppt contour almost 200 km from the mouth of the river to surround the continental islands of Cleveland Bay and Halifax Bay.

Animation 1 shows that the second peak in the flood occurred during NE winds. On day 37, Upstart Bay was almost completely freshwater at the surface and the winds had pushed plume waters into the bay to the south of the mouth of the Burdekin River. Note that the plume waters to the north from the previous peak had mixed with continental shelf water and were diluted further. The second flood event subsided after 10 days and a wind change from the southeast pushed the plume waters northward again. The plume waters from this discharge event eventually hit the mid-shelf reefs between days 51 and 55 with salinity levels down from 35 to 33 ppt. The modelled salinity can be used to determine the degree of mixing and dilution the runoff has undergone, thus the water impacting on the mid-shelf reefs at this time contained approximately 5% freshwater from the runoff of the Burdekin River. Hence the runoff had undergone a 20:1 dilution with ambient seawater by the time it had reached the mid-shelf reefs. By rewinding the animation, it is possible to see that the runoff water took about 18 to 22 days to reach these mid-shelf reefs after leaving the river mouth. Therefore the model simulations also made it possible to scientifically estimate dilutions and time frames for transfers of sediment, nutrients, and contaminants from land runoff to ecosystems such as mid-shelf reefs.

Finally, the third peak in discharge occurred on day 55 after Cyclone Freda passed by offshore heading southward (Puotinen et al., 1997). This passage resulted in strong SE winds that peaked on day 57. These winds exceeded 15 m s^{-1} and were sufficient to vertically mix the plume through the water column to depths exceeding 30 m. The wind also pushed the plume shoreward with some offshore edges retreating 20 to 40 km under these conditions. This produced significant cross-shelf density gradients that resulted in significant cross-shelf transport of the plume once the winds eased. This cross-shelf transport of the plume eventually hit the mid-shelf reefs on day 69 with salinities falling to 32 to 33 ppt at some reefs.

From a management perspective, the model simulations produced by King et al. (1998) identified the fate of the Burdekin River plume in isolation to other river discharges and direct rainfall inputs. This information can provide useful information on catchment management implications of the Burdekin region and its impact on coastal and GBR waters. As an example, Animation 2 also shows the model simulations of the 1981 flood event for the Burdekin, Herbert, Tully, and Johnstone Rivers and it can be seen that the regions of impact from each individual river overlap at times. Further, it can be seen that the movement of the plumes from the smaller rivers are very dependent on the wind force and frequently flow southward with the wind, while the Burdekin's near-field flow is almost always northward due to the Coriolis Force.

Finally, given that the model of King et al. (1998) can reproduce patchiness in the plume, Figure 4 shows a comparison between modelled and measured salinity distributions within the GBR. The left insert in Figure 4 shows the model predicted surface salinity on 27 January, 1981 from discharges from the Burdekin, Herbert, Tully, and Johnstone Rivers. The right insert shows the Wolanski and van Senden (1983) distributions of measured surface salinities collected from 26 and 27 January, 1981. These measured distributions include the direct rainfall and runoff from other smaller rivers within the region including the Haughton, Ross, and Barron Rivers, which are not included in the model predictions. It can be seen from Figure 4 that the model-predicted river plume positions account for many of the features seen in the measured salinity distributions of Wolanski and Van Senden (1983).

SIMULATING THE 1974 FLOOD EVENT

The 1974 simulation depicts the biggest flood of the Burdekin River since 1920 when gauging of the river commenced. Table 1 shows that this event was an extreme event with a likely return period of about 1 in 80 years, based on discharge volume. The flood was continuous for a 4-month period between 17 December, 1973 and 23 April, 1974. Due to the highly active wet season and monsoon activity over the Burdekin catchment area, more than 50 billion tonnes of freshwater poured from this river into the GBR lagoon. The peak discharge exceeded a massive 25,000 tonnes of water per second at times, which resulted in water <26 ppt reaching as far out as Lodestone, John Brewer, and Keeper Reefs. These low salinity events indicate that Burdekin River water can reach the mid-shelf reefs with a dilution rate as low as one part river water to three parts coastal waters.

Toward the end of the flood (Figure 5), all 450 km of inshore waters from Abbot Point in the south to Cairns in the north and through the inter-reef waters of the Central GBR were exposed to waters drained from the Burdekin River catchment. The plume at this time was 25 to 100 km wide.

SIMULATING THE 1991 FLOOD EVENT

The 1991 simulation covers the period from 21 December, 1990 until 8 April, 1991, and included the discharge from the massive amount of rainfall dumped during the passage of Cyclone Joy (Puotinen et al., 1997) and then due to a sustained monsoon activity over the Burdekin catchment area. The total discharge from this flood was the second highest on record (since 1920) and was about 40 billion tonnes of freshwater. The monsoon activity kept the river discharging for 4 months with peak discharge rates exceeding a massive 20,000 tonnes of water per second on two occasions. The first of these peak discharges pushed plume water (<30 ppt) as far offshore as Old and Stanley Reefs (Figure 6). At the time of the second peak discharge, a steady southeast wind change occurred and pushed the plume waters northward, filling Bowling Green Bay, Cleveland Bay, and Halifax Bay with surface waters <30 ppt reaching to the Palm Island group. The plume was eventually pushed all the way along the coast and mid-shelf reefs to Cairns.

SIMULATING THE 1972 FLOOD EVENT

This simulation covers the period from 6 December, 1971 until 22 April, 1972. The total discharge from this flood was about 17 billion tonnes of freshwater. This event included a massive peak discharge of 23,000 tonnes of water per second on 11 January, 1972 due to the passage of cyclone Althea. Afterward a tongue of freshwater (<5 ppt) stretched 60 km to the end of Cape Bowling Green and was sustained for a week. Up to 3 weeks later, a 7.5-m s^{-1} SE wind pushed the plume waters northward with <30 ppt reaching to the Palms Islands.

A third and final downpour of rain over the catchment area started in late February and the river again flooded, this time for a 4-week period. This event occurred during lighter and variable winds, which created a pooling effect around the river mouth. Offshore winds forced the freshwater to mix and drift farther offshore as a patch toward the reefs. A low salinity event (<32 ppt or one part river water to nine parts reef waters) occurred at the mid-shelf reefs after this period of offshore winds and impacted Keeper, Lodestone, John Brewer, and Kelso Reefs (Figure 7).

SIMULATING THE 1979 FLOOD EVENT

This simulation showed a moderate continuous flood of the river from 21 January, 1979 until 16 April, 1979. The total discharge from this flood was over 15 billion tonnes of freshwater. Table 1 shows that this volume corresponds to an event that has an expected annual return period of every 4.9 years.

Toward the end of the flood, 7.5 to 10 m s^{-1} southerly winds pushed the plume waters northward with water about 30 ppt reaching to the Palms (Figure 8). Then on day 67, the plume reached mid-shelf reefs such as Keeper, Lodestone, John Brewer, and Kelso Reef approximately 3 weeks after leaving the river mouth.

MINIMUM SALINITY ANALYSIS OF MODERATE BURDEKIN FLOODS

The minimum salinity predicted at each grid cell of the model was extracted for each wet season to examine the extent of impacts over different years. Two examples of these are shown in Figure 9. From this figure it is possible to observe the spatial variability in plume dynamics from different years. Further, in the "big wet" years already examined (1981, 1974, 1991, 1972, and 1979), their significant discharges ensured that Burdekin plume waters always travelled northward due to Coriolis effects as the river head pushes its way into coastal waters. The discharge volumes of 1983 and 1977 were typical of more common discharge events, calculated to occur once every 2.5 to 3 years (see Table 1). These years all show the characteristic extensive northward movement of the plume in inshore waters. However, the far-field and offshore extent of the plume varies, since it is significantly influenced by the wind patterns that occurred at each time. Indeed, the influence and timing of wind events enabled more Burdekin catchment runoff to be delivered to inshore reefs in years like 1983 and 1977 than some larger floods like 1981. In 1983, the plume took only 14 days to reach Keeper Reef but had diluted significantly (<5% of original runoff water remaining). All other model simulations of the Burdekin River (see McAllister et al., 2000), even low discharge years, show the plume flowed northward after entering coastal waters.

PLUME INTRUSIONS IN THE CAIRNS REGION

In February 2000, moderate flood events occurred from all rivers near Cairns after Cyclone "Steve" passed by. New data collected shortly afterward in the coastal and reef waters offshore of Cairns between 22 and 24 February, 2000 (Figure 10) also demonstrated an intrusion of river plumes into the mid-shelf reefs of the Cairns section of the GBR. The across-shelf transects measured lower salinity water, which appeared to have originated from coastal waters, and intruded into the mid-shelf reef matrix near Norman Reef. The vertical profiles of salinity show that the plume waters have created a stratified water column with lower salinity water at the surface to depths of about 20 m. While this evidence shows that plume intrusions do occur in this region, also, their frequency, intensity, and duration require further investigation.

DISCUSSION

The model simulations of King et al. (2000) and data presented in Wolanski (1994) show that the plume formation from the Burdekin River in flood is significant. When in flood, the Burdekin has been observed to travel over 200 to 400 km to the north in coastal waters due to its discharge strength and wind forcing. The model simulations demonstrate that some of the patchiness in the Burdekin River Plume occurs due to daily variability in the wind field and discharge rates. Steering effects from the coastal topography, continental islands, and the dense reef matrices further create complex spatial patterns in the plume distribution. For smaller rivers such as the Herbert, Tully, and Johnstone systems, plume movements are more variable as wind and local topographic effects tend to dominate plume fate during lower discharge rates.

The simulations also showed that the Burdekin River plume would usually take at least a 2- to 3-week period or more, after discharge from the river mouth, to reach the mid-shelf reefs. Plumes typically reach the bottom in shallow coastal waters (<10 m) although model simulations suggest that strong discharge and wind events will mix plume waters to depths of 30 m at times. In deeper waters, under more moderate conditions, plumes tend to be less dense than surrounding offshore waters. This density difference enables the plume to float buoyantly at the surface and drift with the wind, stratifying the water column. The buoyant plume also continues to spread and mix while on the surface, and has been observed to be 10 to 20 m thick, even through the mid-shelf reef regions.

Under extreme events, such as the flood of 1974, model simulations predicted a low salinity event of 26 ppt at the mid-shelf reefs. Therefore river waters under extreme conditions may reach mid-shelf reefs with a minimum dilution rate of one part river water to three parts coastal seawater.

To date, observations and modelling studies on all river plume dynamics in the GBR have shown that plume trajectories are complex and event-driven. Given the natural temporal and spatial variability and hence patchiness observed in plume behaviour, a risk assessment and return period analysis from many years of observations or model simulations over decades are required to examine the intensity, duration, and frequency of plume impacts in coastal and reef waters of the GBR. King et al. (2000) reported such an analysis for their simulations of the Burdekin alone and the Burdekin, Herbert, Tully, and Johnstone Rivers. This database was ultimately analysed to map the return periods of the likely impacts of runoff from four major rivers to nearby reefs (King et al., 2000; McAllister et al., 2000). While this analysis provides stakeholders with a spatial and temporal risk assessment of river plumes in the central section of the GBR, the risk profile imposed by the other catchments and river systems along the GBR may differ significantly and remain unexplored.

ACKNOWLEDGMENTS

This work was funded by the Cooperative Research Center for the Ecologically Sustainable Development of the Great Barrier Reef (CRC Reef), the Australian Institute of Marine Science (AIMS). The authors acknowledge with thanks the contributions of Dr. Chris Crossland, Dr. Ian Gardiner, Dr. K. Hess, Dr. Janice Lough, Dr. David Barnes, Dr. John Chisholm, Dr. Peter Isdale, Katie Moore, Alan Mitchell, Dr. Miles Furnas, and Dr. Stan Massel.

REFERENCES

Australian Institute of Engineers 1998 *Australian Rainfall and Runoff.* Australian Institute of Engineers Association, Sydney.

Ayukai, T., King, B., & Baird, D. 1997 Hydrographic and nutrient measurements in the Daintree River plume and its vicinity. pp. 35–44 in Steve, A. (ed) *Cyclone Sadie Flood Plumes in the Great Barrier Reef Lagoon: Composition and Consequences.* Great Barrier Reef Marine Park Authority, Townsville, Workshop Series 22.

Hess, K.W. 1986 *Numerical Model of Circulation in Chesapeake Bay and the Continental Shelf.* NOAA Technical Memorandum NESDIS AISC 6. National Environmental Satellite, Data, and Information Service, NOAA, U.S. Department of Commerce, Washington, D.C., 47 pp.

Hess, K.W. 1989 MECCA Program Documentation, NOAA Technical Report NESDIS 46. NOAA, U.S. Department of Commerce, Washington, D.C., 156 pp.

King, B., Spagnol, S., Wolanski, E., & Done, T. 1998 Modeling the mighty Burdekin River in flood. pp. 103–115 in Spaulding, M.L. & Blumberg, A.F. (eds) *Coastal and Estuarine Modeling,* Proceedings of the 5th International Conference, American Society of Civil Engineers, Alexandria, VA.

King, B., McAllister, F., & Done, T. 2000 *Modelling the Impact of the Burdekin, Herbert, Tully and Johnstone River Plumes on the Central Great Barrier Reef.* Final report to the CRC Reef Research Centre from Asia-Pacific Applied Science Associates and the Australian Institute of Marine Science, Townsville.

McAllister, F., King, B., & Done, T. (2000) T*he Database of Predicted River Plume Distributions (1966–1998) in the Central Great Barrier Reef Marine Park—CD ROM and Web Page.* Report to the CRC Reef Research Centre from Asia-Pacific Applied Science Associates and the Australian Institute of Marine Science, Townsville.

O'Neill, J.P., Byron, G.T., & Wright, S.C. 1992 Some physical characteristics and movement of 1991 Fitzroy River flood plume. pp. 36–55 in Byron, G.T. (ed) *Workshop on the Impacts of Flooding.* Great Barrier Reef Marine Park Authority, Townsville, Workshop Series 17.

Puotinen, M.L., Done, T.J., & Skelly, W.C. 1997 *An Atlas of Tropical Cyclones in the Great Barrier Reef Region,* 1969–1997, CRC Reef Research Centre Technical Report No. 19. CRC Reef Research Centre, Townsville, 201 pp.

Wolanski, E. & Ruddick, B. 1981 Water circulation and shelf waves in the northern Great Barrier Reef lagoon. *Australian Journal of Marine and Freshwater Research* 32, 721–740.

Wolanski, E. & Van Senden, D. 1983 Mixing of Burdekin River flood waters in the Great Barrier Reef. *Australian Journal of Marine and Freshwater Research* 34, 49–63.

Wolanski, E. 1994 *Physical Oceanographic Processes of the Great Barrier Reef.* Marine Science Series, CRC Press, Boca Raton, FL, 194 pp.

Wolanski, E., Spagnol, S., King, B., & Ayukai, T. 1997 Patchiness in the Fly River Plume in Torres Strait. *Journal of Marine Systems* 18, 369–381.

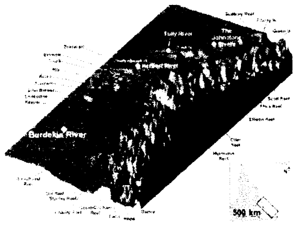

FIGURE 1 Location map of the Burdekin, Herbert, Tully, and Johnstone Rivers and adjacent coastline and a three-dimensional rendered view of the bathymetry and reef matrix of the Central Great Barrier Reef.

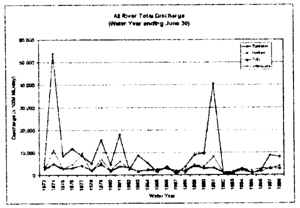

FIGURE 2 Time-series plot of total volume of freshwater discharged by the Burdekin, Herbert, Tully, and Johnstone Rivers for each water year 1972/1973 to 1997/1998.

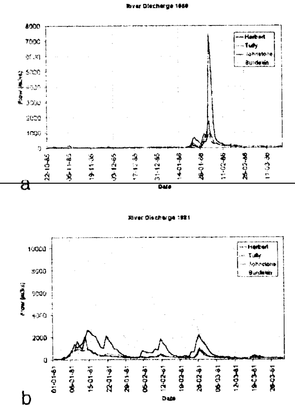

FIGURE 3 The discharge hydrographs (flow rates) for the Burdekin, Herbert, Tully, and Johnstone Rivers for the wet season ending (a) 1986 and (b) 1981 showing the spatial and temporal variability in the flow rates from the major rivers of the Central GBR.

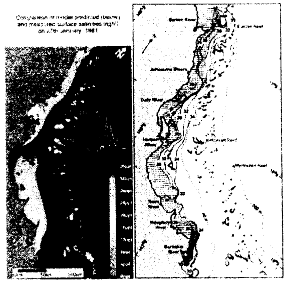

FIGURE 4 Left insert shows the model predicted surface salinity on 27 January, 1981 from discharges from the Burdekin, Herbert, Tully, and Johnstone Rivers. Right insert shows the Wolanski and Van Senden (1983) distributions of measured surface salinities from 26 and 27 January, 1981.

FIGURE 5 A three-dimensional rendered view of the surface salinity distribution immediately following a sustained discharge period over the 1973–1974 wet season. The yellow arrow on the compass represents the wind vector at that time. This plume water is predicted to stretch over 450 km along shelf and at places 100 km offshore.

FIGURE 6 A three-dimensional rendered view of the surface salinity distribution immediately following a sustained discharge period. The insert shows the discharge over the 1990–1991 wet season. The yellow arrow on the compass represents the wind vector at that time. This wind pushed plume water into mid-shelf reef waters over significant distances.

FIGURE 7 A three-dimensional rendered view of the surface salinity distribution immediately following a sustained discharge period. The insert shows the discharge over the 1971–1972 wet season. The yellow arrow on the compass represents the wind vector at that time. This wind pushed plume water into mid-shelf reef waters.

FIGURE 8 A three-dimensional rendered view of the surface salinity distribution immediately following a sustained discharge period. The insert shows the discharge over the 1978–1979 wet season. The yellow arrow on the compass represents the wind vector at that time. This strong offshore wind pushed plume water into mid-shelf reef waters.

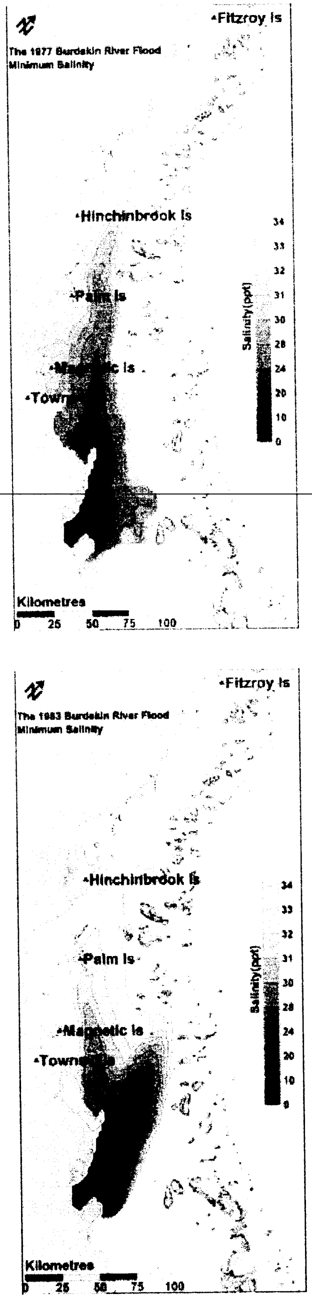

FIGURE 9 Summary distributions of the minimum surface salinity predicted for each grid cell for 1983 and 1977.

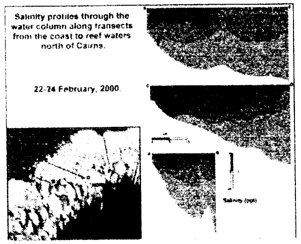

FIGURE 10 Salinity profiles through the water column along the transects shown in the insert from the coast into reef waters offshore of Cairns following the passage of cyclone "Steve" in February 2000.

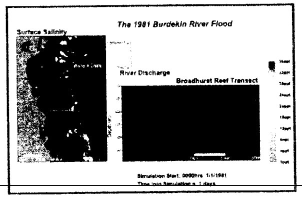

ANIMATION 1 Visualisation of the predicted 1981 Burdekin flood plume using a frame every second day. The left screen shows the surface salinity distribution over the whole model domain. The right screen depicts a vertical slice through the river plume along a transect from Cape Bowling Green to Broadhurst Reef demonstrating its three-dimensional structure in this region. The graph shows the discharge rates over the 1981 wet season (m^3/s) starting from January 1, 1981 and the asterisk indicates the flow rate at the time. The wind vector represents the wind speed and direction at each time.

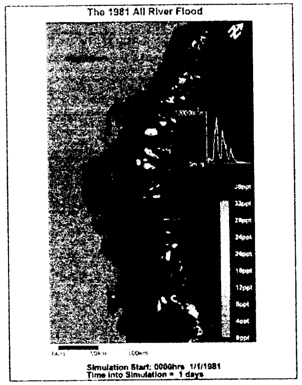

ANIMATION 2 Same as Animation 1 but incorporating also the additional effect of the Herbert, Tully, and Johnstone Rivers.